



HAL
open science

Optical simulation for CMOS imager microlens optimization

Jérôme Vaillant, Flavien Hirigoyen

► **To cite this version:**

Jérôme Vaillant, Flavien Hirigoyen. Optical simulation for CMOS imager microlens optimization. Photonics Europe, SPIE, Sep 2004, Strasbourg, France. pp.200, 10.1117/12.546000 . hal-04514509

HAL Id: hal-04514509

<https://hal.science/hal-04514509>

Submitted on 21 Mar 2024

HAL is a multi-disciplinary open access archive for the deposit and dissemination of scientific research documents, whether they are published or not. The documents may come from teaching and research institutions in France or abroad, or from public or private research centers.

L'archive ouverte pluridisciplinaire **HAL**, est destinée au dépôt et à la diffusion de documents scientifiques de niveau recherche, publiés ou non, émanant des établissements d'enseignement et de recherche français ou étrangers, des laboratoires publics ou privés.

Optical simulation for CMOS imager microlens optimization

Jérôme Vaillant^a and Flavien Hirigoyen^{a,b}

^aSTMicroelectronics, 850 rue Jean Monnet, 38920 Crolles, France;

^bInstitut Fresnel, D.U. St Jérôme, 13013 Marseille, France

ABSTRACT

This paper describes a new methodology we have developed for microlens optimization for CMOS image sensors in order to achieve good optical performances. On one hand, the real pixel is simulated in an optical simulation software and on the other hand simulation results are post-processed with a numerical software.

In a first part, we describe our methodology. We start from the pixel layout description from standard microelectronic CAD software and we generate a three-dimensional model on an optical ray tracing software. This optical model aims to be as realistic as possible taking into account the geometrical shape of all the components of the pixel and the optical properties of the materials. A specific ray source has also been developed to simulate the pixel illumination in real conditions (behind an objective lens). After the optical simulation itself, the results are transferred to another software for more convenient post-processing where we use as photosensitive area a weighted surface determined from the fit of angular response simulation results to the measurements. Using this surface we count the ray density inside the substrate to evaluate the simulated output signal of the sensor.

Then we give some results obtained with that simulation process. At first, the optimization of the microlens parameters for different pixel pitches (from $5.6\mu\text{m}$ to $4\mu\text{m}$). We also have studied the polarization effects inside the pixel. Finally, we compare the measured and the simulated vignetting of the sensor, demonstrating the relevance of our optical simulation process and allowing us to study solutions for a pixel pitch of $3\mu\text{m}$ and less.

Keywords: CMOS image sensor, microlens, optical simulation, microlens design, electro-optical characterization

1. INTRODUCTION

Digital image sensors are more and more present in every day life: digital still cameras, camera phones, webcams, security cameras, etc. This big market follows a main trend which is higher resolution (*i.e.*, larger number of pixels) while keeping small sensors, emphasizing the problem of light collection inside the pixel, mainly for Complementary Metal Oxide Semiconductor (CMOS) technology.¹⁻⁴ In CMOS image sensors, every pixel has its own readout circuit. This embedment involves at least three transistors per pixel, and four transistors per pixel for advanced architectures with enhanced performances. As a consequence, the light-sensitive area (also called photosensitive area) of a pixel is smaller than the pixel itself: for small pixel size it is roughly less than a third of the whole pixel area. This ratio is called the fill-factor of the pixel.

To overcome this loss of sensitivity it is customary to place a microlens on the top of the pixel to concentrate the light to the photosensitive area. This microlens is placed over the CMOS dielectric stack which is made of metallic interconnections insulated by dielectric layers. So the optimal microlens has to concentrate the light on the photosensitive area without losing light by reflection on the metallic wires.⁵ These two constraints depend on the pixel layout (like pixel size and interconnection layout) and on the CMOS process characteristics (like height and type of the dielectric stack). Our objective is to be able to define all the key parameters of the microlens by optical simulation of the pixel, using only the pixel layout and the process properties.

Because there is no optical dedicated simulation software on the standard Computer Aided Design (CAD) platforms for microelectronics, we chose to use a pure optical simulation software and to couple it with the CAD software. The methodology we have developed for that is presented section 2. In this section we detail how the three dimensional model of the pixel is generated from its CAD view, the simulated light source, the optical description of the whole pixel, and finally the extraction of the simulated sensitivities according to the photosensitive areas. In the section 3, we present the first results we have obtained with this simulation methodology: microlens parameters for different pixel pitches, a study of polarization inside the dielectric stack and also a good correlation we have obtained between simulation and vignetting characterization. As a conclusion, we discuss about the next activities on optical simulation mainly focused on overall image sensor performances.

2. METHODOLOGY

The main difficulty we faced when we started the optical simulation of the CMOS image sensor is that there is no optical part on the standard CAD software. This was addressed by choosing an optical ray tracing software for pure optical simulation and then to develop an interface between the microelectronic CAD software and a post-

processing of the simulation with a mathematical computation and analysis software. Our choice was to use Tcl¹ for writing the CAD file conversion scripts, Zemax^{®2} for optical ray tracing, Matlab^{®3} for data formatting and post-processing. On the following sections, we describe the methodology we have developed using these three tools.

2.1. Layout extraction

The first step of this optical simulation methodology is the generation of the model of the sensor. To make this model as realistic as possible, the starting point is the layout of the pixel. This layout is retrieved through a file generated by a CAD software dedicated to microelectronic design. The data of this file have to be translated into a format compatible with the optical simulation software. The CAD tool describes the pixel as a set of polygon for each step of the CMOS process. This tool can generate a text file that gives the coordinates of the vertex of each polygon of each layer. Because we are only interested in the photodiode and the interconnections above the silicon level, we pick out only the relevant layers. This is done with a Tcl script that analyses the text file and creates a table of vertex coordinates for each polygon.

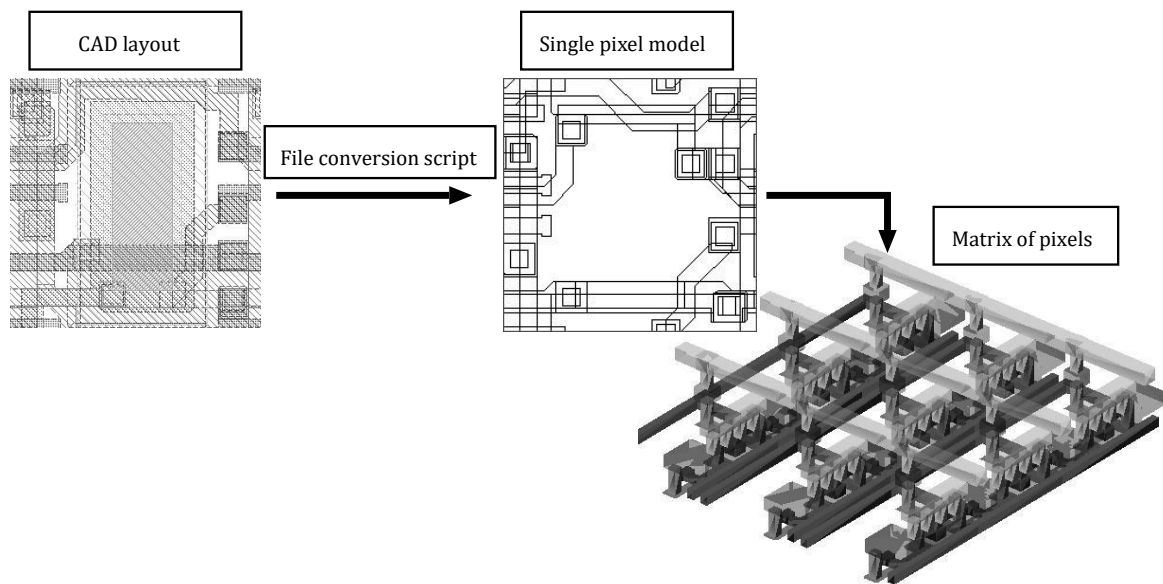


Figure 1. Schematic of the model generation of the pixel from CAD description to three-dimensional optical model of a matrix of pixel.

The next step is to generate the three-dimensional volumes usable in Zemax[®]. In this software, a volume is defined by its faces and these faces must be a collection of elementary triangles or rectangles. So each polygon should be converted as a set of triangles (*i.e.*, triangularized), this is done under Matlab[®]. However, the builtin procedure of triangularization works only with convex polygon and we have both convex and concave ones. So we have developed our own triangularization routine that can handle both convex and concave polygons whatever the orientation of the vertex (clockwise or counterclockwise order). Using the triangularized polygons, we generate the corresponding volume. The height of this volume is given by the CMOS process specification for the given layer (metal layer, via, ...). Then we specify the basic optical properties of the volumes: they could either be reflecting (optional coating could be added on the optical simulator editor), or absorbing or refracting. Finally we write all these data in the Zemax[®] object file format. All these steps are summarized on the figure 1. The last step of the model generation is done under the Zemax[®] editor using the previously defined volumes. For a realistic simulation every pixel of interest must be surrounded by “dummy” pixels. This is mandatory to simulate the right topology for example concerning the parasitic reflections inside the pixel matrix.

2.2. Light shape

In the optical simulator there are many usable light sources but we have to ensure that they reflect our needs. Basically we want to simulate two kinds of light shape: a collimated light and a uniform image area. The first case is mainly used for pixel characterization and is the easiest one: the rays are uniformly distributed over the pixel surface and all the rays have the same direction. For that we use a built-in light source of the optical software. The

¹ <http://www.tcl.tk>

² <http://www.zemax.com>

³ <http://www.mathworks.com>

second case is a little bit more complex: it simulates a pixel looking a uniform surface through an objective. To make it simple we assume the pixel corresponds to a uniform area of the image plane.

It is somewhat difficult to simulate the objective lens and the pixel together. The first problem is a scale problem: the lens is hundred times bigger than the pixel (few millimeters compared to some micrometers). The consequence is that many rays passing through the objective lens will not hit the pixel and then the simulation time will be unnecessarily long. The second problem is that many objective lenses can be used for a same sensor, that means as many simulations as objectives. At the pixel level the rays are distributed uniformly: spatially over the pixel area and angularly inside a cone defined by the exit pupil of the objective and the pixel (see figure 2). The parameters that define the angular distribution are: the f-number of the objective⁴, the field of view of a pixel and the chief ray⁵ angle. Such light shape is not obvious to generate with built-in sources, so we have developed our own source of rays as a dynamically loadable library usable by the ray tracing software. This source follows the user defined parameters f-number, pixel field of view and chief ray angle.

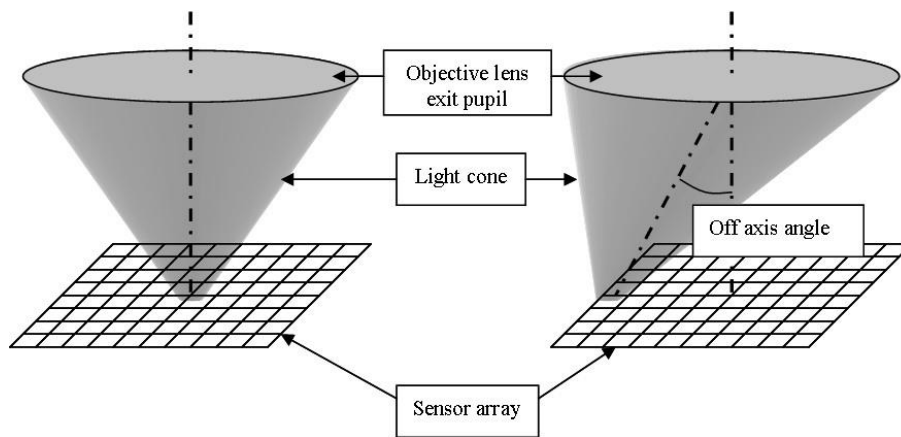


Figure 2. Parameters of the light shape in case of a pixel uniform illumination provided by an objective lens.

2.3. Optical parameters of the model

Once the geometrical elements constituting the pixels have been generated and transferred from the original layout to the optical simulator, a critical aspect is to model their intrinsic optical properties. This can be done by using different modules under the simulator. The difficulty is to put in evidence the optical behavior of these elements which have been firstly designed and optimized to have the best electrical performance.

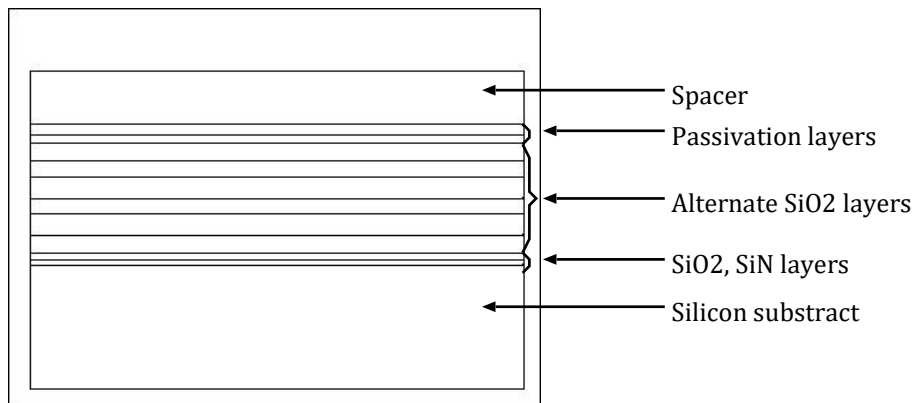


Figure 3. Example of used optical stack: alternate boundaries of oxides placed over silicon substrate.

Following the optical axis we first have the spacer where the filters are placed, then the planarization layers before the alternate SiO₂ layers where are processed the metal levels constituting the pixels. After that we have oxide and nitride silicon. Below that is the silicon substrate where are situated the doping elements constituting the photodiodes and the transistors (see figure 3). On the top of the stack the microlens are placed to focus the light inside the pixel.

⁴ The f-number of an objective is the ratio between its focal length and its exit pupil diameter

⁵ The chief ray is the ray passign through the center of the exit pupil and the center of the pixel of interest

2.3.1. Microlens and filters

These elements are dedicated to focus and filter light. The microlens is a standard plano-convex one with thin edge. The geometrical aspects are set up by defining it as a standard lens in the lens data editor of Zemax® with a positive radius of curvature for the first surface and an infinite radius for the second one which is planar. The optical properties of the material constituting the microlens are defined like for the oxides by creating a new glass from the data of the microlens resin. In the section 3.1 are presented the methodology and the results of the optimization of such a microlens, from the complete pixel model.

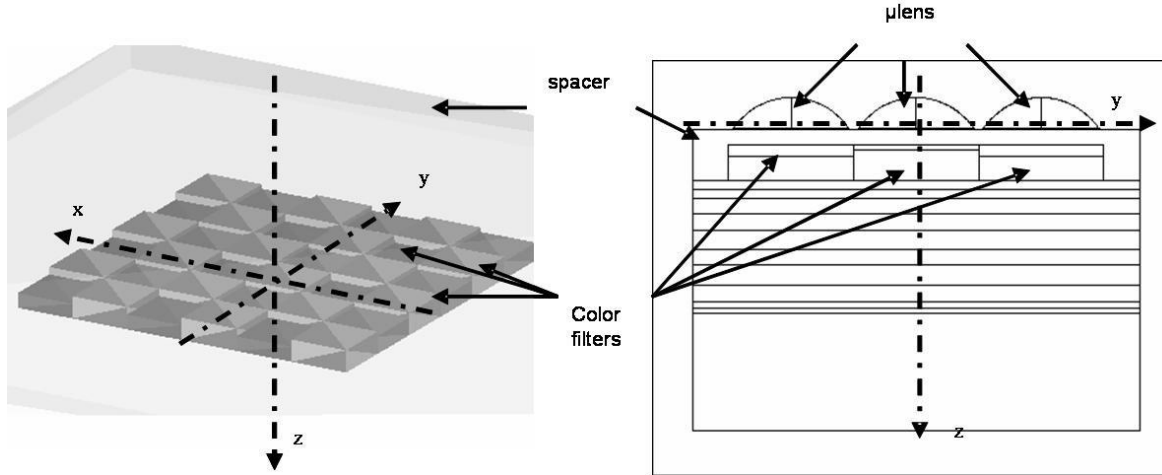


Figure 4. Color filters array design.

The filters correspond to the Bayer pattern dedicated to divide the white light into its three primary colors.

The optical parameters of the three filters (red, green and blue) are measured with an ellipsometer and a spectrophotometer, the critical point being their internal transmittances at visible spectrum.

Those filters are geometrically simulated by rectangular volumes which base dimensions correspond to the pixel size, and which thicknesses correspond to the process. This thickness has to be in accordance with the original one because the filtering parameters depend on the material and on its thickness. The indices and transmittances are set up in the glass catalogue of the simulator for the considered wavelengths (see section 2.3.2 for details), and then we place them inside the spacer (see figure 4).

2.3.2. Oxides

First of all, the pixels interconnections are processed inside alternate oxide stacks. For example each metal is laid inside an insulating stack. These alternate oxide stacks have different mechanical and electrical properties related to the process conditions and to the elements which have to be insulated. As a consequence of it, these properties influence their optical behavior which must be identified and simulated. Each oxide layer is geometrically simulated by a rectangular volume placed in the stack in accordance with the original process.

Once defined from a geometrical point of view, the optical properties of each oxide layer must be defined. We do that by defining a new glass in the glass catalogue of the simulator which optical parameters (refractive index, absorption coefficient) are set up to be the same as the corresponding oxide. These parameters have been measured for all oxide types with an ellipsometer at the visible spectrum, from 200nm to 800nm each 5nm.

Thus, for a given oxide the indices are entered in the index data editor of the glass catalogue. Then the simulator computes the fit of these index data to a dispersion formula. We achieve a good fit using the Schott formula:

$$n^2 = a_0 + a_1\lambda^2 + a_2\lambda^{-2} + a_3\lambda^{-4} + a_6\lambda^{-8} \quad (1)$$

The parameters of fit computation are the a_i factors. When the glass catalogue is completed, the simulator is able to compute the refraction angle of each simulated analysis ray passing through each interlayer by solving the Descartes equation:

$$n_i \sin(\theta_i) = n_r \sin(\theta_r) \quad (2)$$

with n_i , θ_i , n_r , θ_r the refraction index and the angle in incident and refractive layer respectively. The energetic aspects are computed using indices and absorption coefficients. Like for the refractive index we enter in the transmittance data editor the internal transmittance calculated from the measurements of absorption for a given thickness with

a spectro-photometer. From these transmittances, Zemax® calculates the corresponding absorption coefficient from Beer's law:

$$IT = e^{-\alpha\tau} \quad (3)$$

with IT the internal transmittance, τ the corresponding thickness and α the absorption coefficient. Now the oxides are completely defined, in a geometrical and optical way, and we will use this model to make an energetic status of the oxide stack by simulating the power transmittance of a polarized monochromatic wave passing through it. The results of this study are exposed in the section 3.2.

2.3.3. Pixel interconnections

After having correctly placed the constituting elements of the pixels inside the oxide stacks, we have to set up their optical properties. In a simpler way regarding the oxide layers, we will define these elements as perfect mirrors, transparent or totally absorbing.

The mirror-like objects are the metallic elements such as metal levels, contacts and vias. This property means that the simulator computes the refraction angle of each analysis ray hitting the surface of such an object equal to the incident one. To be more realistic according to the process we defined anti-reflective top-coats on faces of certain elements which are still active in the visible. The characteristics of these top-coats are defined by ASCII files. In our case, we enter the real and imaginary indices with the associated wavelength, and the thickness of the corresponding top coat. In the editor of Zemax® we define the top-coats on the concerned faces of such elements. Then the simulator is able to compute the attenuation effects due to this top-coat by linearly interpolate the entered data.

The transparent or absorbing objects are the polysilicon elements. In a first approximation we consider the unsalicyded ones as totally transparent in the visible, the others being considered as 100% opaque to the visible. We simply have to set the material of such objects as absorbing or transparent with the right refractive index.

2.4. Photosensitive area definition

Using the model of the pixel and the light source described previously, we are able to obtain a ray density anywhere inside the model. To extract the simulated sensitivity of the pixel we defined three surfaces corresponding to the original layout. The two first one are the central and the peripheral parts of the photodiode, the perimeter of the third one is defined as the equidistance from the photodiode to the surrounding MOS transistors. We want to model the density of probability of the photo-generated electrons collection by a weighted sum of these three surfaces. To determine these weights we fit the simulated angular response of the pixel to the corresponding measurement, for vertical and horizontal angles of incidence (relative to pixel layout). Our assumption is that the weights are only dependent of the process, so for each process we did one fit using all data (related to all pixel architectures). The figure 5 shows the result of the weighted photosensitive surface and the resulting fit for a given pixel angular response. Once the photosensitive surface has been determined, we used it for all next simulations dedicated to evaluate the image sensor performances (see section 3).

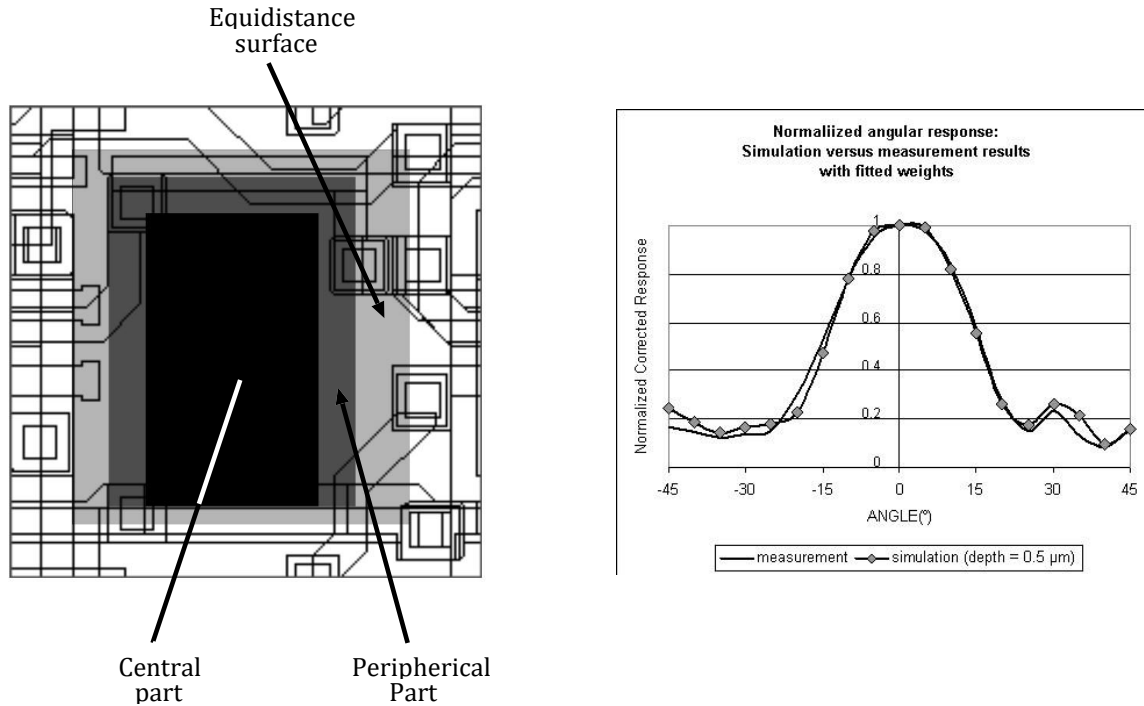


Figure 5. Layout of the photosensitive surface as a weighted sum of central and peripheral part of the photodiode, and equidistance surface. The graph shows the result of the fit of the weights on measurement.

With all the previous components of the optical simulation, we run the ray tracing itself. To control the accuracy of the simulation, we do five runs of ray tracing with basically one hundred thousand rays per pixel. Then we verify that the simulation results are not dispersed from run to run. If the dispersion is more than a few percents, the number of rays launch per run is not sufficient and must be increased.

3. RESULTS

3.1. Microlens optimization

The first goal of the optical model is to use it to optimize the microlens parameters specifications in accordance with the feasibility of the industrial process. For that our methodology is to use the optimization modules of Zemax® in the sequential mode of the simulator with the oxide model. In that way the parameters are optimized in a geometrical point of view. Then we place the obtained microlens on the complete pixel model and we optimize it from the previous specificities according to a user-defined routine under the non-sequential mode.

The sequential mode is a well-suited mode for the optimization of imaging systems. The analysis rays computed by the simulator hit each surface of the model once and only once in a predetermined sequence, that means that no multiple reflections between two surfaces are simulated. In this mode, the model is simple (only surfaces representing the oxide stacks), numerically fast and we can use automatic optimization algorithms to obtain the parameters of the microlens. The process imposes to us to optimize a plano-convex microlens with thin edge, so the entry variable is the radius of curvature, the edge microlens thickness being set to zero, and its diameter being fixed by the process and the pixel pitch.

Once this done we import the sequentially optimized parameters of the microlens and use it on the complete pixel model (microlens + oxide stacks + filters + pixels) under the non-sequential mode. This mode takes into account the multiple reflections of the analysis rays and their energetic aspects, which are useful for a radiometric approach of the optimization. Here the optimization is done by maximizing the sensitivity of the detector positioned under the considered pixel and by minimizing the sensitivity of the neighborhood detectors (minimization of cross-talk). For that we minimize a merit function which is the quadratic sum of the difference between the target values and the current values weighted by a certain factor:

$$MF = \frac{\sum_i g_{u_i} (u_i - c_i)^2}{\sum_i g_{u_i}} \quad (4)$$

where MF is the Merit Function, g_{u_i} are the weights, u_i are target values and c_i current values. Here our target values are 1 for the normalized sensitivity and 0 for the sum of the neighborhood sensitivities (cross-talk), their

corresponding weights being fixed to 1. The variable is still the radius of curvature, the microlens thickness being calculated at the beginning of each optimization step as follows:

$$h = r \left[1 - \sqrt{1 - \left(\frac{d}{2r} \right)^2} \right]^2 \quad (5)$$

with d the microlens diameter, r the radius of curvature and h the microlens thickness (see figure 6).

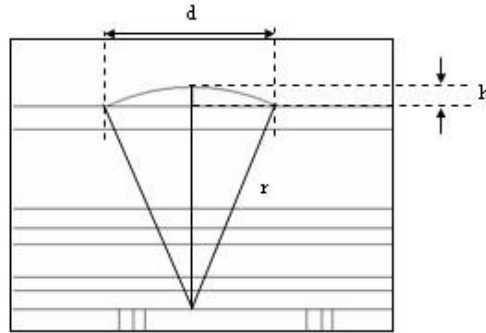


Figure 6. Definition of the microlens parameters used for the optimization.

The figure 7 shows an optimized microlens, focusing a collimated beam on the substrate and the following table gives the specificities of microlens for two pixel pitches:

Pixel pitch	Microlens diameter	Radius of curvature	Microlens thickness
$5.6\mu m$	$5.2\mu m$	$4.0\mu m$	$1.1\mu m$
$4.0\mu m$	$3.6\mu m$	$4.2\mu m$	$0.4\mu m$

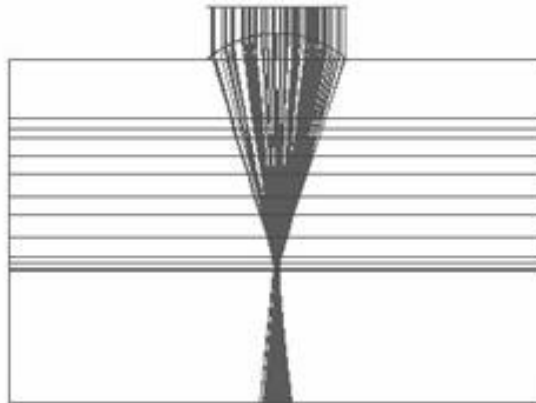


Figure 7. Optimized microlens under collimated beam illumination.

3.2. Polarization effects on dielectric stacks study

Here the idea is to make a status of the energetic attenuation the light undergoes by passing through the oxide stacks. For that we use the non-sequential mode, the model with oxide stacks and the optimized microlens. We illuminate it with a collimated beam at 532 nm and examine the collected energy for incident angles varying from 0° to 45° , for Transverse Electric mode (TE), Transverse Magnetic mode (TM), and for randomly polarized waves.

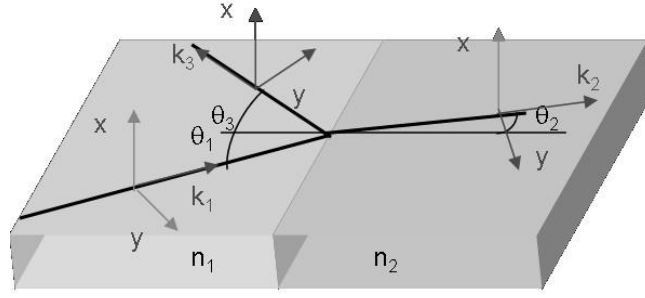


Figure 8. Reflection and refraction at the boundary between two dielectric media

Using Fresnel theory, we can see effects of the polarization by studying the reflection and refraction of a monochromatic plane at a planar boundary between two dielectric medias (figure 8): part of this wave will be refracted and reflected.

To quantify the part of the incident wave that is reflected or refracted, we have to calculate the power reflectance (R) and transmission (T). These values are the squares of the absolute value of the reflection (r) and transmission (t) coefficients, for the x-polarized mode (TE) and the y-polarized mode (TM). In that case, the reflection and transmission coefficients satisfy the Fresnel equations:

$$\begin{aligned}
 r_{TE} &= \frac{n_1 \cos \theta_1 - n_2 \cos \theta_2}{n_1 \cos \theta_1 + n_2 \cos \theta_2} & r_{TM} &= \frac{n_2 \cos \theta_1 - n_1 \cos \theta_2}{n_2 \cos \theta_1 + n_1 \cos \theta_2} \\
 R_{TE} &= |r_{TE}|^2 & R_{TM} &= |r_{TM}|^2 \\
 T_{TE} &= 1 - R_{TE} & T_{TM} &= 1 - R_{TM}
 \end{aligned} \tag{6}$$

After having verified the accuracy of the results given by the model for the TE and TM modes used on the oxide stacks regarding the theory, we used that model to see the energetic attenuation on TE, TM and randomly polarized waves as a function of the angle of the incident collimated beam (see figure 9).

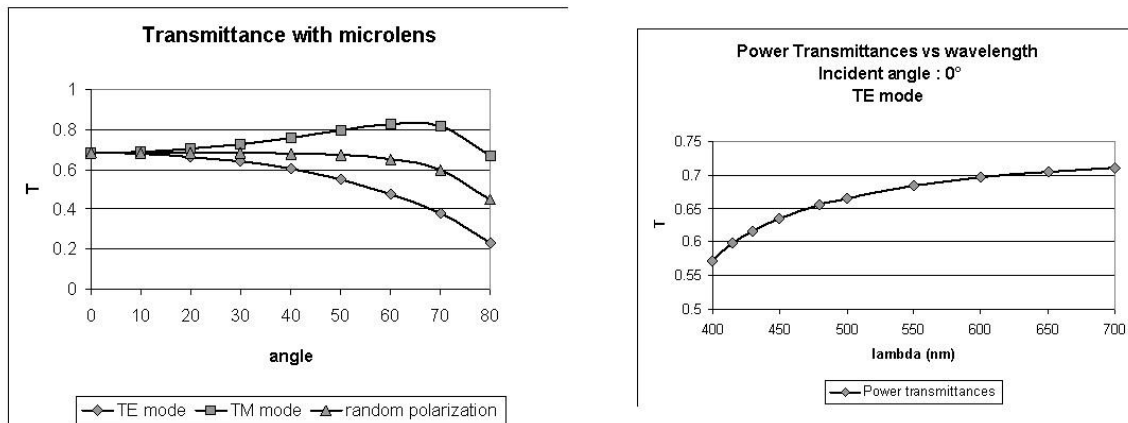


Figure 9. Attenuation results at 532 nm and power transmittance versus wavelength at 0 for TE modes.

From this study we conclude that for a randomly polarized wave at 532 nm, we have a contribution of attenuation as follows: *i)* 15% of loss due to the oxide/oxide diopters, *ii)* 15% of loss due to the oxide/substrate diopter, *iii)* a negligible loss due to the microlens. After having verified that we have a rather constant attenuation from 0° to 50°, we can make a chromatic study at 0° for the TE polarization. From the simulation results we can say that the polarization of the light will induce a constant loss of 30% (red) to 45% (blue) whatever incident angle we consider (as long as the field of view does not exceed 50°).

3.3. Vignetting effect study: simulation versus characterization results

Now we look at the vignetting effect due to the important angle of incidence of the chief ray angle on the border of the sensor⁶ (see figure 2). For that we simulate the sensitivity of the pixel at the center and at the edge of the die using the previously described model and light source. This simulation allowed us to see the origin of the vignetting: it is to be due to a shift of the spot at the silicon level. On the first hand, this spot is focused outside of the photosensitive area, and on the other hand the metallic interconnections shade the light reducing the number of incoming rays (see figure 10-b).

Once these origins have been identified we have used our simulation methodology to reduce the vignetting by optimizing the position of the microlens versus the pixel position in the sensor matrix (see figure 10-c). Then we have processed test chips with these optimized microlenses for a $4\mu\text{m}$ pixel pitch. The characterization and the corresponding simulations of the un-optimized and the optimized sensor have been done and compared. The following table summarizes the relative illumination results. This quantity, related to the vignetting, is defined by the ratio between the edge pixel sensitivity and the center one of the sensor.

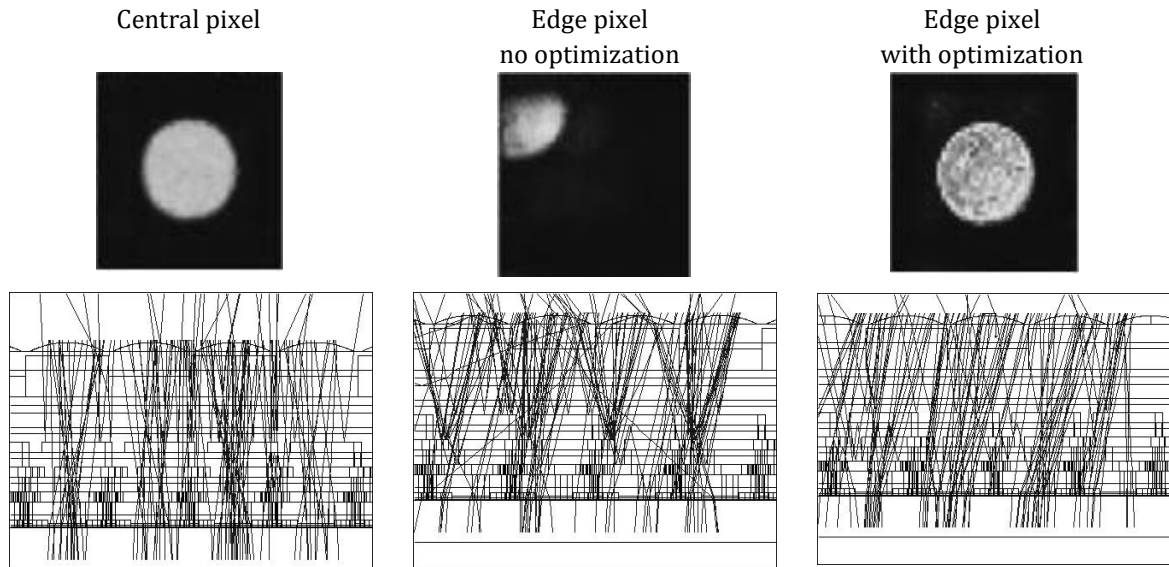


Figure 10. Vignetting effect, ray density and ray tracing at the center of the sensor (a), at the edge without optimization of the microlens position (b) and at the edge with microlens optimization (c).

Chief ray angle	12°	16°	22°	microlens type
Simulation	70%	44%	42%	Un-optimized
Measurement	71%	47%	42%	
Simulation	96%	88%	91%	Optimized
Measurement	100%	87%	93%	

The good correlation between our simulation results and the characterization measurements make us confident of our simulation methodology. Its efficiency is emphasized by the strong improvement of relative illumination we get by optimizing the position of the microlens with the simulator. This allows us to work further on the optical performances of the image sensor and more specifically on microlens improvement.

4. CONCLUSION

In this paper we have presented a methodology we have developed at STMicroelectronics for the optical simulation of the pixel. This goal has been achieved by combining different software allowing us to go from pixel layout description to the light density inside the silicon. This density is then post-processed to give us the simulated sensitivity of the pixel. This whole procedure has been calibrated by fitting the simulated and measured angular responses of different pixels.

Using this methodology we were able to define the parameters of the microlens for the different pixel sizes (from $5.6\mu\text{m}$ to $4\mu\text{m}$) developed at STMicroelectronics. A study of polarization inside the pixel has also been done showing the attenuation due to the alternate oxide boundaries in the stack. We have considered this attenuation acceptable for a reasonable range of angles of incidence (0° to 50°). After these fundamental studies we focused on the sensor performance under real illumination through the vignetting study. At first, we have verified the correlation of our simulation results with the corresponding measurements in the un-optimized case. Once the model qualified, we used it to optimize the microlens position in the sensor matrix in order to reduce the vignetting. The obtained solution has been confirmed by measurement of this optimized-microlenses solution. Based on these encouraging results, we will put in evidence other overall sensor performance limitations and use the described methodology to select the best pixel architecture as new light collection solution for highly integrated CMOS image sensors (*i.e.*, pixel pitch of $3\mu\text{m}$ and smaller).

ACKNOWLEDGMENTS

We want to thank all the STMicroelectronics and Institut Fresnel people that have been involved in this project for their help and advices.

REFERENCES

1. E. Fossum, "Active pixel sensors: Are ccd's dinosaurs?," in *Charge-Coupled Devices and Solid State Optical Sensors III*, M. M. Blouke, ed., **1900**, pp. 2–14, SPIE, July 1993.
2. J. Janesick, "Lux transfer: complementary metal oxide semiconductors versus charge-coupled devices," *Optical engineering* **41**, pp. 1203–1215, June 2002.
3. E. Fossum, "Cmos image sensors: Electronic camera-on-a-chip," *IEEE Transactions on electron devices* **44**, pp. 1689–1698, October 1997.
4. T. Chen, P. B. Catrysse, A. El Gamal, and B. A. Wandell, "How small should pixel size be?," in *Sensors and Camera Systems for Scientific, Industrial, and Digital Photography Applications*, M. M. Blouke, N. Sampat, G. M. Williams, and T. Yeh, eds., pp. 451–459, SPIE, SPIE, may 2000.
5. H.-J. Hsu, F.-T. Weng, C.-K. Chang, and Y.-H. Hsiao, "Microlens design for compact lens system," in *Smart Sensors, Actuators, and MEMS*, J.-C. Chiao, V. Varadan, and Can'e, eds., **5116**, pp. 640–646, SPIE, 2003.
6. P. B. Catrysse, X. Liu, and A. El Gamal, "Qe reduction due to pixel vignetting in cmos image sensors," in *Sensors and Camera Systems for Scientific, Industrial, and Digital Photography Applications*, M. M. Blouke, N. Sampat, and T. Williams, George M. and Yeh, eds., pp. 420–430, SPIE, may 2000. Vol. 3965.